

Combined GPS and InSAR Models of Postseismic Deformation from the Northridge Earthquake

Andrea Donnellan

Jet Propulsion Laboratory,
California Institute of Technology,
4800 Oak Grove Drive

Pasadena, California, USA

e-mail: donnellan@jpl.nasa.gov,

phone +1-818-354-4737,

fax: +1-818-393-5471,

University of Southern California,

Los Angeles, California

USA.

Jay W. Parker

Jet Propulsion Laboratory,
California Institute of Technology,
4800 Oak Grove Drive

Pasadena, California, USA

e-mail: Jay.W.Parker@jpl.nasa.gov,

phone +1-818-354-6790,

fax: +1-818-393-4965

Gilles Peltzer,

Jet Propulsion Laboratory,
California Institute of Technology,
4800 Oak Grove Drive

Pasadena, California, USA

e-mail: Gilles.F.Peltzer@jpl.nasa.gov ,

phone +1-818-354-7539,

fax: +1-818-354-9476

University of California

Los Angeles

e-mail: mailto:peltzer@ess.ucla.edu

phone +1-310-206-2156

Abstract

Models of combined Global Positioning System (GPS) and Interferometric Synthetic Aperture Radar (InSAR) data collected in the region of the Northridge earthquake indicate that significant afterslip on the main fault occurred following the earthquake. Additional shallow deformation occurred to the west of the main rupture plane. Both datasets are consistent with logarithmic time-dependent behavior following the earthquake indicative of afterslip rather than postseismic relaxation. Aftershocks account for only about 10% of the postseismic motion. The two datasets are complimentary in determining the postseismic processes. Fault afterslip and shallow deformation dominate the deformation field in the two years following the earthquake. Lower crustal deformation may play an important role later in the earthquake cycle.

Introduction

California is well instrumented with GPS and seismic instruments and serves as an excellent laboratory for studying the complete earthquake cycle. The 1994 Northridge earthquake provides an excellent opportunity for determining postseismic processes for several reasons. The earthquake occurred within a GPS network being used to measure shortening across the Ventura basin (Figure 1). InSAR data were collected less than two months before the Northridge earthquake and two years following the earthquake, making for an excellent comparison between GPS and InSAR observations. The Northridge earthquake occurred on a buried thrust fault resulting in vertical postseismic motions that make it possible to discriminate between fault afterslip and lower crustal relaxation.

GPS analysis techniques have now improved to the point that daily absolute horizontal and vertical positions can be determined to 3 and 8 mm respectively (Zumberge et al., 1997). Using continuous data, horizontal velocities accurate to 1 mm/yr can be achieved in 5 years (Argus and Heflin, 1995). Campaign style measurements can yield velocities accurate to 3–5 mm/yr over two years (Donnellan and Lyzenga, 1998) and to better than 2 mm/yr over longer timespans (Shen et al., 1996). Semi-continuous or frequent measurements collected following the earthquake indicate a time-dependent postseismic signal that decays within two years of the earthquake.

The technique of radar interferometry consists of combining Synthetic Aperture Radar (SAR) images of the same area acquired from repeated passes on a given orbit to extract the interferometric phase, which provides for each pixel of the scene a measure of the antenna-ground path length difference between the two images. After appropriate corrections for orbit configuration and topography, the interferometric phase depicts the line of sight component of the surface displacement that occurred during the time interval covered by the two images (Gabriel et al., 1989). The technique has been successfully applied to map the surface displacement field related to earthquakes (e.g., Massonet et al., 1993; Zebker et al., 1994; Peltzer et al., 1998) and surface strain related to post-seismic relaxation processes (e.g., Peltzer et al., 1996; Peltzer et al., 1998). The main error on the line of sight displacement estimate comes from variations in the phase propagation delay through the troposphere (e.g., Goldstein, 1995; Zebker et al., 1997). Such a signal does not generally exceed a phase cycle (28 mm of line of sight change) in the Los Angeles area.

GPS results from campaign and continuous SCIGN data indicate that a narrow band of shortening runs along the front of the Transverse Ranges through the Ventura and northern Los Angeles basins (Donnellan et al., 1993; Argus et al., 1999). The shortening rates are 7–10 mm/yr and 5–6 mm/yr for the Ventura and Los Angeles basins respectively. Analysis of the data shows nearly pure shortening indicating thrust faulting environments.

Forward and inverse elastic modeling, when combined with geologic data, have been useful in estimating fault slip rate and geometry for the Ventura basin. The Northridge earthquake occurred along the southeastern portion of the basin on a fault similar to that defined by elastic forward models. While the slip rate and geometry of the faults can be well-described by elastic models the fault locking depths are shallower than the local earthquakes. Viscoelastic finite element models in which a ductile lower crust relaxes between earthquakes and the basin is

composed of compliant sediments explains the concentrated strain rates and deep seismogenic depths (Hager et al., 1999). In the following discussion elastic models seem to adequately describe the postseismic deformation occurring in the two years following the Northridge earthquake. Viscous deformation is likely to have a longer response time and probably dominates later.

Post Northridge Results

GPS data collected following the Northridge earthquake show significant postseismic deformation on the order of 30% of the deformation produced by the mainshock (Donnellan and Lyzenga, 1998). Aftershocks show a similar sense of motion as the GPS results, but only account for about 10% of the measured motions, suggesting that at least 90% of the postseismic motion has occurred aseismically (Donnellan and Lyzenga, 1998). The GPS data are consistent with afterslip on the main rupture plane, but also suggest shallow deformation to the west. InSAR measurements provide an independent measurement of postseismic deformation associated with the Northridge earthquake.

The Northridge earthquake occurred while the European Space Agency ERS-1 satellite was operating in a 3-day repeat mode, which was not providing global coverage of the surface of the Earth at low latitudes. The first post-seismic ERS data acquisitions of the area of Northridge were possible after March, 1995, when the satellite was placed again on a 35-day repeat cycle. The interferogram we use in this study covers the 11/8/1993–12/6/1995 time interval, thus including both the co-seismic displacement signal and the signal associated with 2 years of post-seismic deformation (Figure 2a). The time period is close to the time period of the GPS data. The SAR data correlate well in the San Fernando Valley where much of the deformation from the Northridge earthquake took place. Decorrelation occurs in the hills to

the north of the valley. SAR observations are present at the locations of the GPS stations, although an unwrapping error causes the value at CSUN to be suspect.

To analyze the post-seismic deformation we removed from the interferogram a modeled phase corresponding to the co-seismic signal (Figure 2b). We used the variable slip distribution model determined by inversion of seismic and geodetic data by Wald et al. (1996). The residual phase (Figure 2c) depicts, in principle, surface displacements related to post-seismic processes but also includes incorrectly modeled co-seismic displacements. The results match qualitatively well where the InSAR signal does not decorrelate (Figure 2d). To assess the validity of the approach, we first compared the displacement observed with InSAR data at GPS sites with the post-seismic displacement measured with the GPS instruments.

We fit a linear trend to the GPS data, however, sites closer to the rupture plane show a clear nonlinear postseismic trend. The observable postseismic transients decay with time with most of the motion occurring within the first year after the earthquake. The horizontal and vertical postseismic motions, at stations where they are significant, can be fit by both exponential decay and logarithmic functions. Models of the GPS results indicate that afterslip, consistent with a logarithmic decay (Marone et al., 1991), is the dominant mechanism in the two years following the earthquake (Donnellan and Lyzenga, 1998). Because the GPS data were sampled nonuniformly and infrequently and the InSAR data were only sampled twice a constant velocity fit to the data is the most reasonable way to model the dominant postseismic process using all of the available data. Additionally for sites more than one fault dimension the errors are large enough that it is difficult to discriminate between linear and nonlinear trends in the data.

Since the InSAR and GPS data do not cover the exact same time intervals, we scaled the InSAR data to be compatible with the GPS velocities. We removed the coseismic signal (Wald et al., 1996) from the InSAR data, and then scaled the InSAR by the best exponential and logarithmic fit functions of the GPS data (Figure 3). The first GPS observations were made about 3 days after the Northridge earthquake, and substantial afterslip may have occurred during that time. Coseismic offsets calculated from the GPS observations are consistently larger than those of the Wald et al. (1996) model, which is based largely on seismic observations, suggesting a fair amount of immediate postseismic deformation. We tested for the best scaled fit of the InSAR data (e.g. with or without rapid postseismic deformation for different models) for the time intervals 1/17/94–12/6/95 and from 1/20/94–12/6/95. We correlated the line-of-sight (LOS) station displacements calculated from the GPS solutions with the LOS displacements observed with InSAR at those locations. The best correlation is for the

logarithmic afterslip model scaled from three days after the mainshock to December 1995. This model takes into account rapid postseismic deformation. The InSAR displacement is relative and since the reference site RCAG is not in the radar frame, the InSAR measurements can be shifted arbitrarily. There is likely an unwrapping problem near site CSUN, which, if solved, may shift it by -2.8 cm or -5.6 cm. Afterslip is best fit by a logarithmic function, which is consistent with the inversions of just the GPS data that suggest that afterslip was the dominant mechanism in the first two years following the earthquake. Models of viscoelastic relaxation (exponential decay) or slip on the downdip extension of the fault do not fit well. A particular problem with exponential relaxation is that the sites over the rupture plane should show subsidence, but the observed results show about 12 cm of uplift, which is consistent with afterslip.

Friction Rate Parameters

The calculated logarithmic function that fits the data can be used to estimate friction parameters for the Northridge fault. The initial coseismic slip rate for the thickness-averaged region undergoing afterslip is 174 mm/day, which is within the range of that observed for the Superstition Hills earthquake. The friction rate parameter is about 0.002 which matches laboratory values for poorly consolidated materials (C. Marone, written communication, June 1998).

Inversions

The GPS and postseismic InSAR observations are qualitatively similar. We see deformation over the rupture plane and to the west of the rupture. The magnitude of the deformation is also similar in both cases. Because both the correlation between the GPS and InSAR data and the inversions of the GPS data strongly point toward fault afterslip following the earthquake we

used the InSAR data to improve the inversion, particularly west of the rupture plane (Figure 2d). The inversion code is based on Okada's (1985) methods for a dislocation in an isotropic elastic medium. The inversion model uses a residual-minimization procedure based on a downhill simplex simulated annealing algorithm (Donnellan and Lyzenga, 1998), for which 9 fault parameters can be solved (location, depth, dip, length, width, slip).

The results for the main fault plane are nearly identical to those observed with the GPS only solution (Table 4), further indicating that afterslip was the dominant mechanism following the earthquake. By adding the InSAR data we were able to free every parameter for the auxiliary fault plane. In the combined solution the potency, or moment, is about a factor of 1.8 greater than in the GPS only solution. The size of the fault patch is about one third the size of the fault patch in the GPS only solution, while the amount of slip on the fault is substantially greater (Figure 4). The depth to the top of the "fault" is slightly deeper. The amount of slip at depth on this auxiliary fault is about 50 cm, which while large is probably not unreasonable. A qualitative look at the InSAR results shows very localized deformation west of the mainshock rupture suggesting that displacement on a long planar structure in this region is likely. The residuals indicate that the model is consistent with the data, particularly for the GPS data (Figure 5).

Table 1

Fault Parameters for Combined and GPS Only Inversions

Parameter	Combined		GPS Only	
	<i>Main Plane</i>	<i>Auxiliary Plane</i>	<i>Main Plane</i>	<i>Auxiliary Plane</i>
X (km)	7.7 ± 0.5	-6.4 ± 0.7	8.8 ± 1.3	-5.6 ± 0.3
Y (km)	13.0 ± 1.0	12.7 ± 0.3	12.8 ± 1.9	13.3 ± 1.1
Strike (°)	300.0	286.6 ± 3.0	300.0	277.8
dip (°)	40.0	54.0 ± 7.7	40.0	38.0
depth (km)	7.3 ± 1.0	0.5 ± 0.6	5.3 ± 1.5	0.1 ± 0.7
width (km)	18.8	5.2 ± 1.2	18.8	8.6
length (km)	12.1	13.1 ± 1.1	12.1	23.0
strike-slip (mm/yr)	25.5 ± 22.4	-308.9 ± 97.1	36.0 ± 30.2	-12.1 ± 22.2
dip-slip (mm/yr)	276.0 ± 40.5	413.3 ± 107.0	203.3 ± 59.4	93.8 ± 53.4

Table 1. Fault Parameters for Combined and GPS Only Inversions. The models shown here represent typical inversions but are nonunique. The GPS and combined GPS/InSAR models are in good agreement for the fit to the main rupture plane. The greater sampling of the InSAR to the west of the rupture area improves the fit for the auxiliary plane. The combined model should be taken as a qualitative example fit. The errors are difficult to assess due to lack of a rigorous error model on the InSAR data, errors in the coseismic model, and varying sampling intervals of the InSAR data. The X and Y coordinates are east and north distances, respectively, of the north-east (upper right) corner of the plane from the epicenter of the Northridge earthquake (N34.20883, W118.54067). Depth is to the top of the fault plane. Positive strike-slip component indicates left-lateral motion, and positive dip-slip indicates thrust motion. Errors are 1σ and are not scaled by the χ^2/dof .

As previously reported, the auxiliary fault does not correspond to any mapped fault but may rather be indicative of general deformation of the upper crust as a result of the mainshock. This "fault," which is more likely representative of broad deformation in the upper crust, coincides with shallow aftershocks that are also interpreted as deformation of a quasi-elastic material (Unruh et al., 1997).

The reported χ^2/dof for the combined inversion is 0.3. However, it is highly sensitive to the assumed SAR "uncertainty". That assumed uncertainty is partly arbitrary because the SAR data are scaled in such a way that the few GPS results have comparable weight in the inversion to the heavily sampled SAR data. The SAR uncertainties include largely systematics like model removal and flattening, and are far from white. The dominant source of that error is most certainly highly correlated systematics, therefore we do not scale the formal reported errors.

Conclusions

Both GPS and InSAR data collected in association with the Northridge earthquake indicate that a significant amount of afterslip occurred on the mainshock plane in the two years following the earthquake. In addition, a significant amount of localized deformation occurred to the west of the fault plane, which can not be linked to a mapped fault. The results imply that the upper crust near Northridge is inhomogeneous and contains localizations of softer material, or bedding plane faults. Future observations will indicate if afterslip ceases and other mechanisms, such as viscoelastic relaxation of the lower crust, begin to dominate later in the earthquake cycle.

Acknowledgments

This work was carried out at the Jet Propulsion Laboratory, California Institute of Technology, under contract with NASA. Support was also provided by the U.S. Geological Survey and National Science Foundation through the National Earthquake Hazards Reduction Program (NEHRP) and the Southern California Earthquake Center (SCEC). SCEC is funded by NSF Cooperative Agreement EAR-8920136 and USGS Cooperative Agreements 14-08-0001-A0899 and 1434-HQ-97AG01718. The SCEC contribution number for this paper is 398

References

- Argus D.F., Heflin, M.B., Donnellan, A., Webb, F.H., Dong, D., Hurst, K.S., Jefferson, D.C., Lyzenga, G.A., Watkins, M.M., Zumberge, J.F., (1999), Shortening and thickening of metropolitan Los Angeles measured and inferred by using geodesy, *Geology*, 27, 703–706.
- Argus, D.F., and Heflin, M.B., (1995) Plate motion and crustal deformation estimated with geodetic data from the global positioning system, *Geophys. Res. Lett.*, 15, 1973–1976.
- Donnellan, A., and Lyzenga, G.A., (1998), GPS observations of fault afterslip and upper crustal deformation following the Northridge earthquake, *J. Geophys. Res.*, 103, 21,285–21,297.
- Donnellan, A., Hager, B.H., King, R.W., and Herring, T.A., (1993), Geodetic measurement of deformation in the Ventura basin region, southern California, *J. Geophys. Res.*, 98, 21,727–21,739.
- Gabriel, A.G., Goldstein, R.M., and Zebker, H.A., (1989), Mapping small elevation changes over large areas: Differential radar interferometry, *J. Geophys. Res.*, 94, 9183–9191.
- Goldstein, R., (1995), Atmospheric limitations to repeat-track radar interferometry, *Geophys. Res. Lett.*, 22, 2517–2520.
- Hager B.H., Lyzenga, G.A., Donnellan, A., Dong, D., (1999), Reconciling rapid strain accumulation with deep seismogenic fault planes in the Ventura basin, California, *J. Geophys. Res.*, 104, 25,207–25,219.
- Marone, C.J., Scholz, C.H., and Bilham, R., (1991), On the mechanics of earthquake afterslip, *J. Geophys. Res.*, 96, 8441–8452.
- Massonnet, D., Rossi, M., Carmona, C., Adragna, F., Peltzer, G., Feigl, K., and Rabaut, T., (1993), The displacement field of the Landers earthquake mapped by radar interferometry, *Nature*, 364, 138–142.
- Okada, Y., (1985), Surface deformation due to shear and tensile faults in a half-space, *Bull. Seim. Soc. Am.*, 75, 1135–1154.
- Peltzer, G., Rosen, P., Rogez, F., and Hudnut, K., (1996), Postseismic rebound in fault stepovers caused by pore fluid flow, *Science*, 273, 1202–1204.
- Peltzer, G., Rosen, P., Rogez, F., and Hudnut, K., (1998), Poroelastic rebound along the Landers 1992 earthquake surface rupture, *J. Geophys. Res.*, 103, 30,131–30,145.
- Shen, Z., Jackson, D.D., and Ge, B.X., (1996), Crustal deformation across and beyond the Los Angeles basin from geodetic measurements, *J. Geophys. Res.*, 101, 27,957–27,980.
- Unruh, J.R., Twiss, R.J. and Hauksson, E., (1997), Kinematics of post-seismic relaxation from aftershock focal mechanisms of the 1994 Northridge, California earthquake, *J. Geophys. Res.*, 102, 24,589–24603.
- Wald, D.J., Heaton, T.H., Hudnut, K.W., (1996), The slip history of the 1994 Northridge, California, earthquake determined from strong-motion, teleseismic, GPS, and leveling data, *Bull. Seim. Soc. Am.*, 86, S49–S70.
- Zebker H.A., Rosen, P.A., and Hensley, S., (1997), Atmospheric effects in interferometric synthetic aperture radar surface deformation and topography maps, *J. Geophys. Res.*, 102, 7547–7563.
- Zebker, H. A., Rosen, P., Goldstein, R.M., Gabriel, A., and Werner, C.L., (1994), On the derivation of coseismic displacement fields using differential radar interferometry: the Landers earthquake, *J. Geophys. Res.*, 99, 19,617–19,634.
- Zumberge, J.F., Heflin, M.B., Jefferson, D.C., Watkins, M.M. and Webb, F.H., (1997), Precise point positioning for the efficient and robust analysis of GPS data from large networks, *J. Geophys. Res.*, 102, 5005–5017.

Figure 1

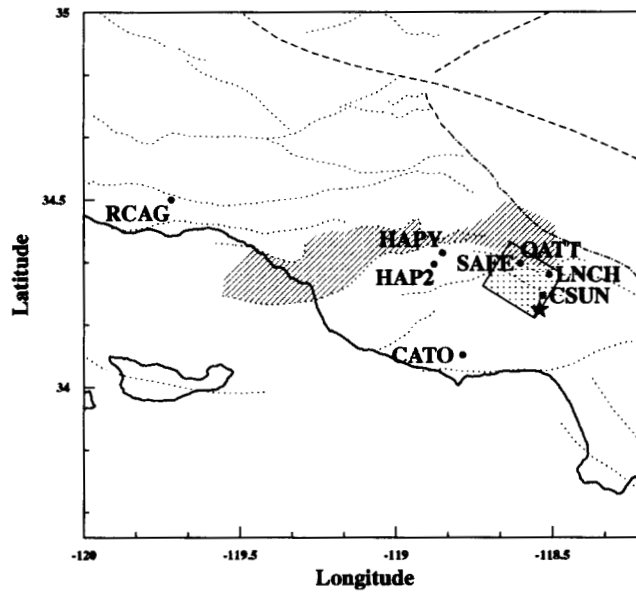


Figure 1. Location of the GPS stations. The coastline is marked by the heavy line. The Ventura basin is shaded. The epicenter of the Northridge earthquake is marked by a star and the shaded rectangle indicates the rupture area.

Figure 2

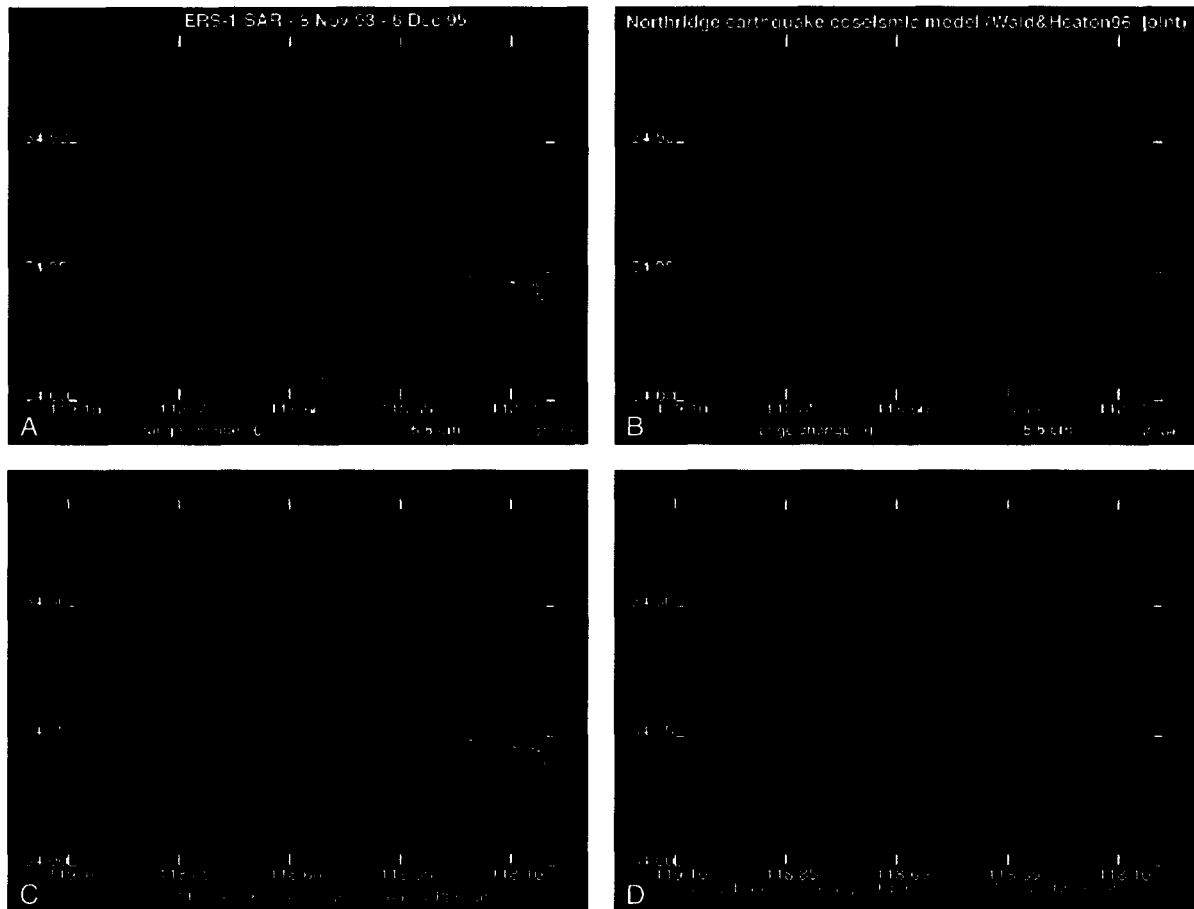


Figure 2. A) Observed interferogram for the time period November 1993 – December 1995. B) modeled phase corresponding to the co-seismic signal. C) Residual interferogram after removal of the coseismic signal. D) Modeled phase from the best fit postseismic inversion.

Figure 3

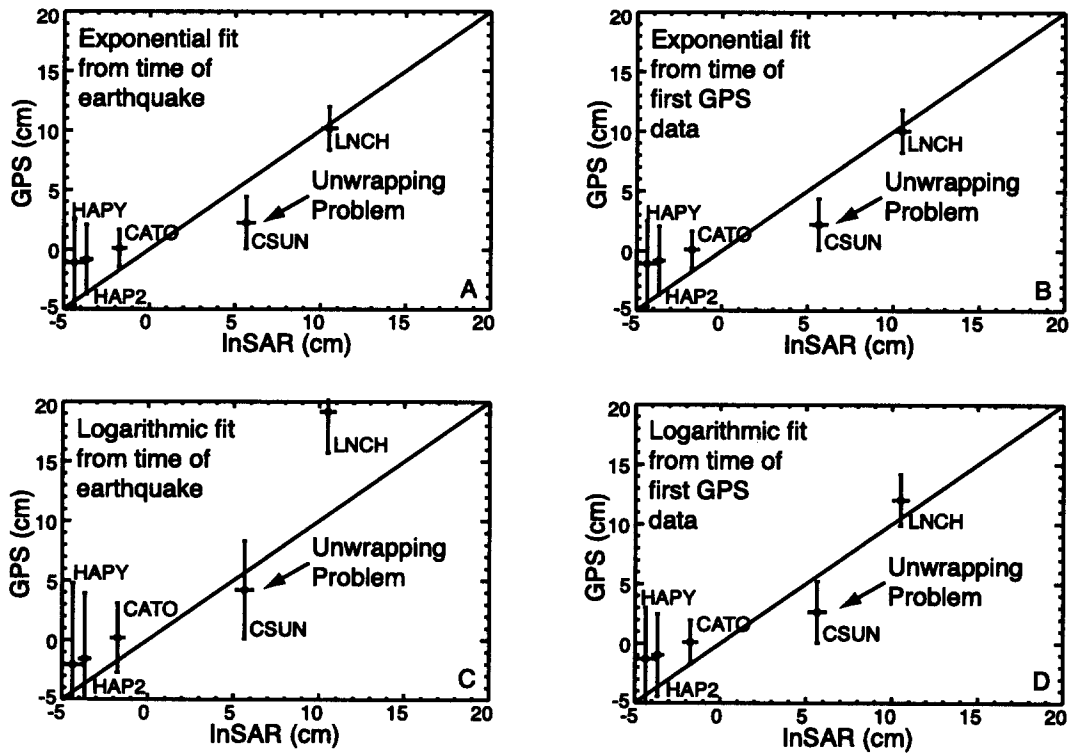


Figure 3. Correlation between GPS and InSAR for various assumptions on the style of postseismic motion.

Figure 4

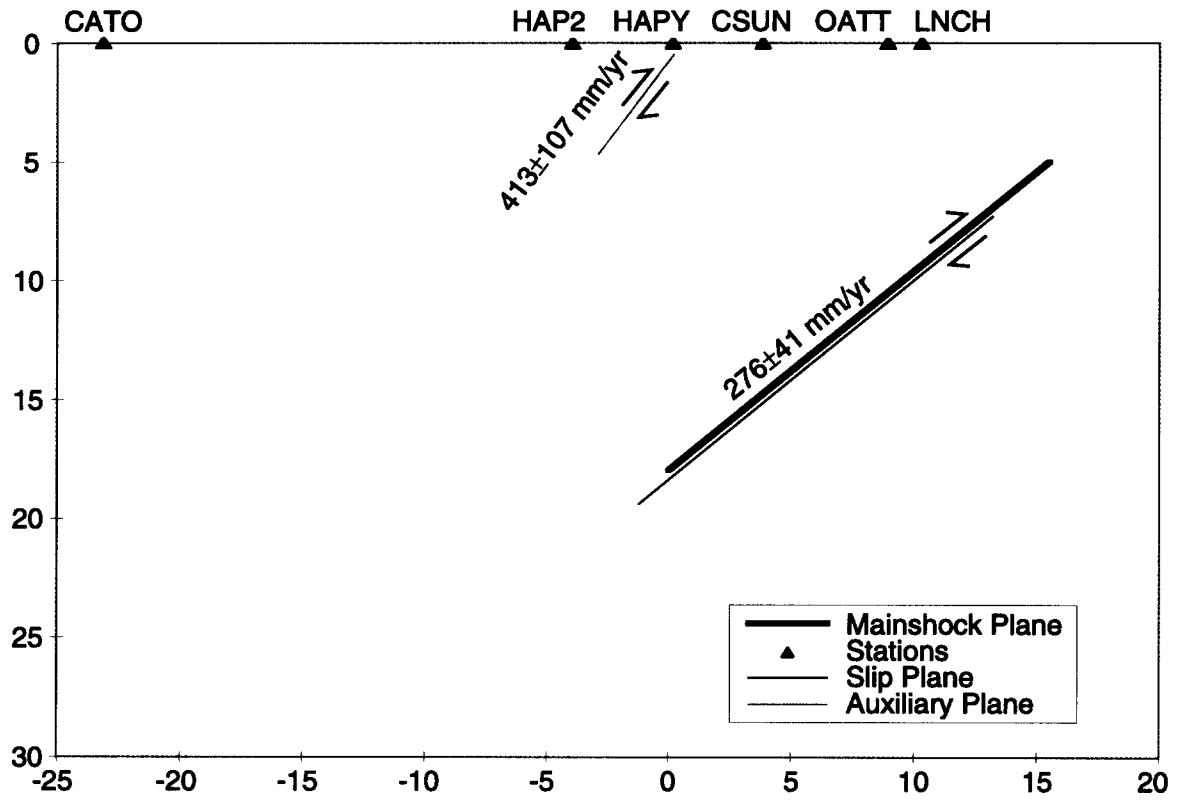


Figure 4. Cross-section showing mainshock rupture plane and calculated faults.